

**A PAC ANALYSIS OF THE MANLIUS-COEYMANS FORMATIONAL  
BOUNDARY HELDERBERG GROUP OF NEW YORK STATE**

---

**A Thesis Submitted  
to the Temple University Graduate Board**

---

**in Partial Fulfillment  
of the Requirement for the Degree**

**MASTER OF ARTS**

---

by

**William M. Goodman**

**April 1985**

**DEPARTMENT COPY**

**A PAC ANALYSIS OF THE MANLIUS-COEYMANS FORMATIONAL  
BOUNDARY HELDERBERG GROUP OF NEW YORK STATE**

---

A Thesis Submitted  
to the Temple University Graduate Board

---

in Partial Fulfillment  
of the Requirement for the Degree

**MASTER OF ARTS**

---

by

William M. Goodman

April 1985

**DEPARTMENT COPY**

A PAC ANALYSIS OF THE  
MANLIUS-COEYMANS FORMATIONAL BOUNDARY  
HELDERBERG GROUP OF NEW YORK STATE

William M. Goodman

A thesis submitted in partial fulfillment  
of the requirements for the degree of  
Master of Arts in Geology, College of  
Arts and Sciences, Temple University  
Philadelphia, Pennsylvania

April, 1985

*E. J. Anderson*

Dr. Edwin J. Anderson

\_\_\_\_\_  
Date

*Peter W. Goodwin*

Dr. Peter W. Goodwin

\_\_\_\_\_  
Date

## ACKNOWLEDGEMENTS

I wish to extend my thanks to the Temple University Geology Department staff.

Special thanks are extended to the following faculty members:

Dr. Anderson and Dr. Goodwin for their guidance in conducting fieldwork and in organizing and writing this thesis.  
Dr. Myer for taking the time to critically review this manuscript.

I would like to thank the following people who have helped in so many ways:

Randy and Mildred for all their help in cutting through red tape, particularly at the end;

Terry O'Reilly for photographic work and consultation;

David Hassrick of AGES Corporation whose interest in PACs kept me moving toward completion of this project;

and particularly to Larry Saraka for dealing with me as a roommate, classmate and field partner at the same time;

I would also like to thank Pete Goodwin, Terry O'Reilly, and the entire student body of the department, graduate and undergraduate, past and present, who have made my academic and social endeavors during my time at Temple so rewarding.

Finally, I would like to thank Temple University for the financial support that made this project possible.

### Dedication

This thesis is dedicated to my family with love. Their support remained unwaivering throughout the extent of this project.

## TABLE OF CONTENTS

	PAGE
I. INTRODUCTION.....	1
Previous Interpretations of the Manlius-Coeymans Boundary.....	1
Objectives.....	10
Methods.....	13
II. MANLIUS FACIES AND PALEOENVIRONMENTS.....	15
III. MANLIUS PACS	
General Characteristics of Upper Thacher PACs.....	35
PACs in Columnar Section.....	37
IV. PAC CORRELATIONS.....	44
V. THE MANLIUS-COEYMANS FORMATIONAL BOUNDARY.....	54
VI. CONCLUSIONS.....	70
VII. APPENDIX: FIELD GUIDES TO LOCALITIES.....	71
VIII. BIBLIOGRAPHY.....	73

## LIST OF FIGURES

<u>FIGURES</u>	PAGE
1. Rickard's stratigraphic framework for the Helderberg Group of New York State.....	2
2. The Manlius-Coeymans unconformity as contended by early workers.....	4
3. Application of gradualistic concepts to the Helderberg Group.....	7
4a. Schematic representation of the ravinement process.....	9
4b. Ravinement concept as applied to the Manlius-Coeymans boundary by Anderson.....	9
5. Diagrammatic representation of fundamental tenets of the PAC hypothesis.....	11
6. Comparison of the time-stratigraphic nature of PACs with the diachroneity of traditional stratigraphic units.....	12
7. Correlation of columnar sections, upper Thacher Member of the Manlius Formation.....	inside back cover
8. Legend for facies represented in stratigraphic columns.....	17
9a. Field photograph of supratidal birdseye mud facies, PAC 7 at Kingston.....	19
9b. Thin-section photonegative of supratidal birdseye mud facies, PAC 6 at North Catskill.....	19
10a. Field photograph of cryptalgal laminite facies, PAC 8 at Cherry Valley.....	20

10b.	Thin-section photonegative of cryptalgal laminite facies, PAC 8 at South Catskill.....	20
11a.	Field photograph of ostracode calcarenite facies, PAC 5 at Schoharie.....	23
11b.	Thin-section photonegative of ostracode cal- carenite facies, PAC 9 at Cherry Valley.....	23
12a.	Field photograph of ribbon bed facies, PAC 5 at Thacher Park.....	25
12b.	Thin-section photonegative of ribbon bed facies, PAC 8 at Schoharie	
13a.	Field photograph of stromatoporoid biostrome facies, PAC 10 at New Salem.....	28
13b.	Thin-section photonegative of stromatoporoid biostrome facies, PAC 7 at New Salem.....	28
14a.	Field photograph of thin-bedded calcarenite facies, PAC 7 at North Catskill.....	30
14b.	Thin-section photonegative of thin-bedded calcarenite facies, PAC 7 at East Kingston.....	30
15a.	Field photograph of medium-bedded calcarenite facies, PAC 10 at Callanan Quarry.....	32
15b.	Thin-section photonegative of medium-bedded calcarenite facies, PAC 11 at Cherry Valley.....	32
16.	Field photograph of strophomenid "coquina" bed, top of PAC 11 at Schoharie.....	34
17.	Field photograph of subtidal-to supratidal PAC, PAC 8 at Thacher Park.....	36



18. Field photograph of fully subtidal PAC,  
PAC 10 at Schoharie.....38
19. Stratigraphic column and interpreted relative  
water-depth curve for upper Thacher section  
at Thacher Park.....40
20. Field photograph of transition from strophomenid-  
bearing calcarenite to crinoidal calcarenite  
across the formational boundary at Thacher Park...43
21. Field photograph of two algal laminite  
horizons in the Thacher at South Catskill.....45
22. Field photograph of PAC 8 algal laminite  
horizon at Cherry Valley.....46
23. Field photograph of PAC 8 algal laminite  
horizon at Schoharie.....46
24. Field photograph of the PAC 8 algal laminite  
horizon at New Salem.....47
25. Field photograph of the PAC 8 algal laminite  
horizon at Climax Quarry.....47
26. Field photograph of PAC 8 algal laminite  
horizon at North Catskill.....48
27. Field photograph of the PAC 8 algal laminite  
horizon at Kingston.....48
28. Stratigraphic column and interpreted relative  
water-depth curve for upper Thacher section  
at South Catskill.....50
29. Correlation of upper Thacher sequence by

	comparison of patterns in the magnitude punctuation events.....	52
30.	Field photograph of v-shaped solution pits on the formational boundary at South Wilbur.....	55
31.	Field photograph of solution cavities in the uppermost Thacher beds at North Catskill....	56
32.	Field photograph of upper Thacher section at Cherry Valley.....	58
33.	Field photograph of Manlius PACs 9 and 10 at Thacher Park.....	59
34.	Field photograph of Manlius PACs 9 and 10 at New Salem.....	61
35.	Thin-section photonegative of Manlius-derived clast in basal Coeymans bed at New Salem.....	61
36.	Field photograph of strophomenid-bearing medium-bedded calcarenite, PAC 10 at Climax Quarry.....	63
37.	Field photograph of the upper Thacher section at North Catskill.....	64
38.	Field photograph of Manlius-Coeymans formational boundary at Kingston.....	66
39.	Close-up field photograph of Manlius-Coeymans formational boundary at Kingston.....	66
40.	Field photograph of Manlius-Coeymans formational boundary at South Wilbur.....	67
41.	Stratigraphic relationships between upper Thacher PACs and overlying Coeymans Formation.....	68

## ABSTRACT

Application of the PAC hypothesis to the Thacher Member of the Manlius Formation has resulted in its division into eleven correlative PACs, shallowing-upward cycles produced by sedimentary aggradation following rapid episodic base-level rises. The eleven Thacher PACs are organized into two sequences. Manlius PACs 1-5 contain predominantly intertidal facies; Manlius PACs 6-11 are comprised mainly of subtidal and supratidal facies. These sequences are discernible at all localities in the Hudson Valley and central New York State.

This study demonstrates that certain distinctive facies found in PACs of the upper Thacher sequence developed laterally persistent horizons, an observation made earlier by Rickard (1962). The PAC 8 algal laminite horizon, which corresponds to the waterlime datum of Rickard (1962, figure 2), provides the primary time and environmental datum for the upper Thacher PAC sequence.

Correlation of upper Thacher PACs demonstrates that the Manlius-Coeymans formational contact is unconformable in eastern New York State. The thickness of section and number of PACs in the upper Thacher decreases progressively from west to east. Erosion responsible for the missing section and PACs is attributed to differential tectonic uplift of the eastern basin margin prior to any Coeymans deposition.

## INTRODUCTION

The purpose of this study is to apply the principles and methods of the PAC hypothesis to a detailed analysis of the Manlius-Coeymans boundary. This formational contact has been variously interpreted as a major unconformity, a depositional contact and a ravinement, each interpretation a product of gradualistic stratigraphic assumptions. In this study, the Manlius-Coeymans boundary is analyzed from an episodic perspective.

Previous Interpretations of the Manlius-Coeymans Boundary

Jaanusson (1960, p. 221) recognized discontinuities in limestones as distinct surfaces which "show signs of etching, boring activities of organisms, or both". He cited many examples of disconformities from the stratigraphic records of Europe and North America. From Jaanusson's description of the erosional surfaces, the following list of some features indicative of discontinuities can be compiled: 1) solution pits or other karstic features on the boundary surface; 2) bleached zones below sharp contacts; 3) concentrations of iron or phosphatic compounds on the boundary surface; 4) wedging out of part of a succession in one direction; 5) intraformational conglomerates; 6) encrusting of organisms on the boundary surface.

The presence of many of these features at the Manlius-Coeymans formational boundary in the Helderberg Group of New York State (figure 1) has not been sufficient evidence for universal acceptance of this surface as a disconformable

Figure 1:  
Stratigraphic framework of the Helderberg  
Group in eastern New York State. After  
Rickard (1962).

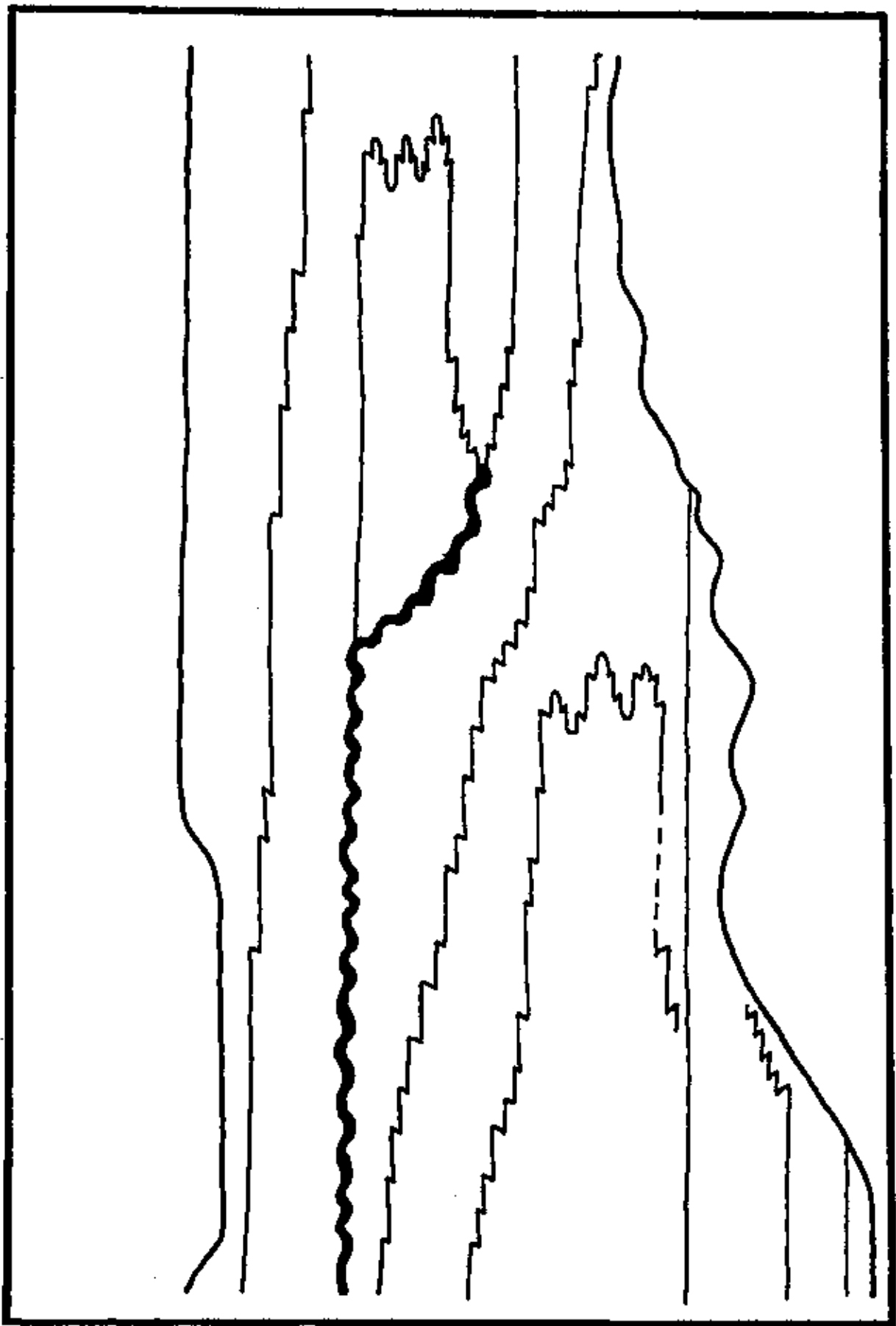


contact. Over the past fifty years, opinion regarding the nature of this surface has vacillated coincidentally with changes in the basic assumptions which underlie prevalent stratigraphic theories. Early researchers, working under the premise that each Helderberg formation is contemporaneous throughout its extent (reviewed by Rickard, (1962, p. 104), contended that the Manlius-Coeymans boundary marks a significant unconformity (figure 2). The absence of younger Manlius members in eastern New York and the wavy, irregular nature of the contact in the Hudson Valley were cited as evidence of large-scale erosion. Logie (1933) noticed that several feet of the uppermost Manlius (Thacher Member) were missing at some localities in the Catskill and Saugerties quadrangles. Chadwick (1944, p. 152) reported slabs of Manlius rock up to a yard or more in length "caught up" in the Coeymans two to three feet above the contact at localities north of Catskill.

The "layer cake" approach of early workers was abandoned by later workers, who following the actualism of Walther, envisioned formations to be the products of "facies-areas", or depositional environments, which have migrated over time with gradual changes in sea-level. Consequently, the notion that each Helderberg formation represents an isochronous, basin-wide environment gave way to the idea that these formations are time-transgressive deposits of once laterally contiguous paleoenvironments. This new concept was based primarily upon observation of the juxtaposition of modern sedimentary environments. Accordingly,

Figure 2:  
Large-scale unconformity at the Manlius-  
Coeymans contact as contended by early  
workers.





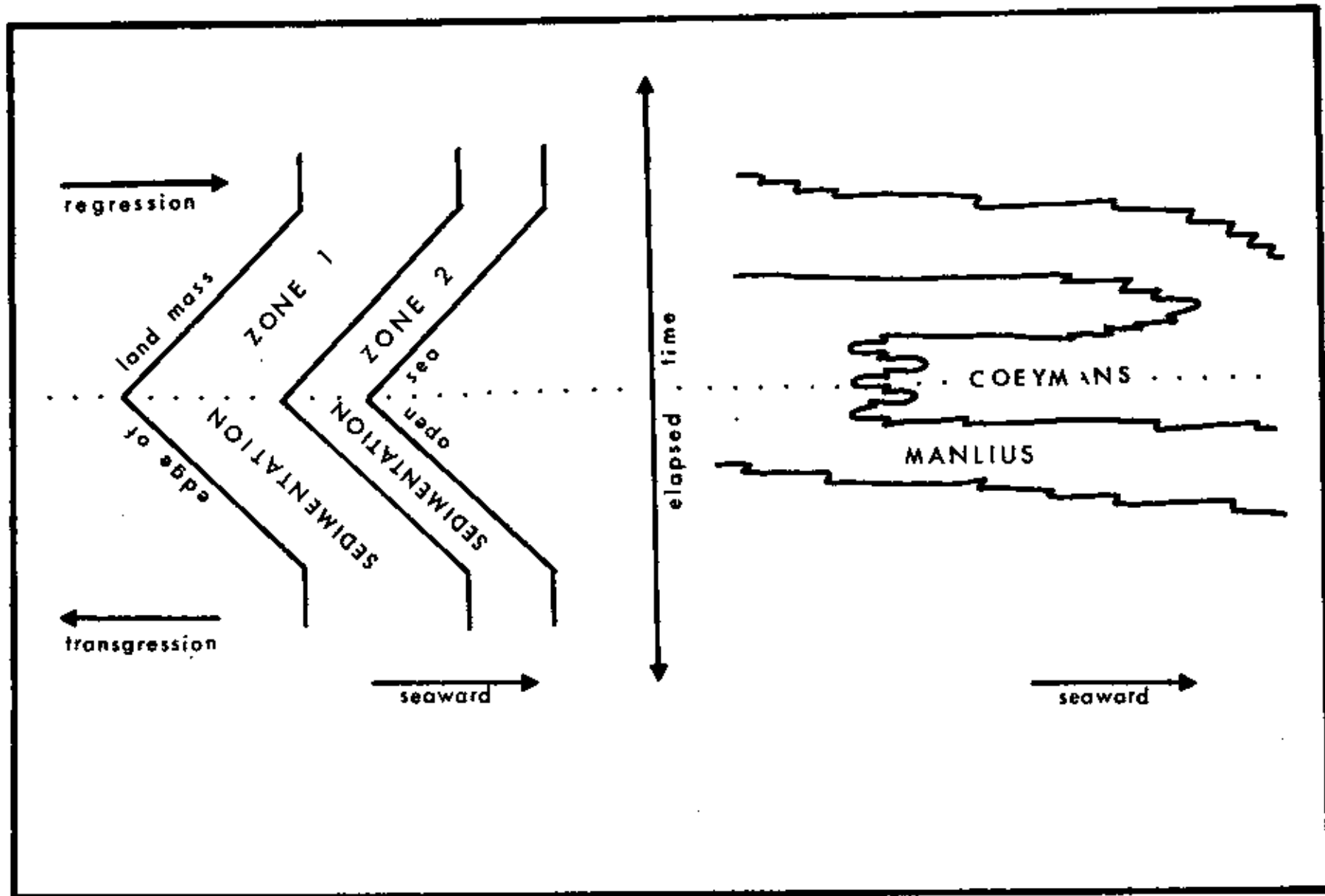
the differences in lithology between formations of the Helderberg Group have been thought to reflect the variation in facies observed in a transect from onshore to offshore in modern carbonate environments.

Consistent with these new assumptions, Davis (1953, p. 27), after a stratigraphic analysis of the Manlius-Coeymans formational boundary in central New York State, concluded that although minor local disconformities attributable to oscillating conditions of deposition may exist at the contact, there was no hiatus between Manlius and Coeymans deposition. Rickard (1962, p. 101), in his definitive reconstruction of Upper Cayugan and Helderbergian stratigraphic relationships for New York State, suggested that in view of the inferred environments in which each facies (formation) was deposited, the possibility that all could have existed contemporaneously in an advancing sea is a strong one. He refuted evidence for the unconformity at the Manlius-Coeymans boundary proposed by early workers by demonstrating that the younger Manlius members grade laterally into the Coeymans and Kalkberg Formations in the Hudson Valley. Rickard's conclusion that the Olney and younger members were never deposited in eastern New York greatly reduces the magnitude of the unconformity required to explain the configuration of Helderberg formations. Consequently, Rickard (1962, p. 49) concluded that any erosion occurring at the formational contact in the Hudson Valley is attributable to "the advance of somewhat deeper, better agitated waters into an

area previously occupied by relatively shallow, quiet waters."

In support of Rickard's interpretations and consistent with the deductive models of Shaw (1964) and Irwin (1965), Laporte (1969) interpreted the Helderberg Group as a transgressive carbonate sequence deposited continuously within a shallow epeiric sea. Laporte (1969, p. 117) concluded that the Manlius, Coeymans, Kalkberg and New Scotland Formations, representing supratidal through below-wave-base subtidal environments, developed contemporaneously in a generally west to east direction across a shallow epicontinental sea. According to Laporte, slow gradual transgression of the Helderberg sea occurring simultaneously with regional subsidence permitted the accumulation and northwest secular migration of facies belts (formations) across central New York producing a vertical stratigraphy which today records the lateral pattern of depositional environments which existed in the Helderberg Basin (figure 3). According to this interpretation, the Manlius-Coeymans formational boundary represents the migration of a near-wave-base shelf environment over a restricted lagoon and tidal flat environment. Arguing against the supposed disconformity at the contact, Laporte (1967, p. 95-96) concluded that "the presence of Manlius-derived intralasts within the Coeymans...indicates that parts of the Manlius were indurated and eroded during early Coeymans deposition", and the time intervals between subaerial exposure and subsequent reworking could have been geologically very short.

Figure 3:  
Application of the gradualistic concepts of  
Shaw (1964) and Irwin (1965) to the Helder-  
berg Group

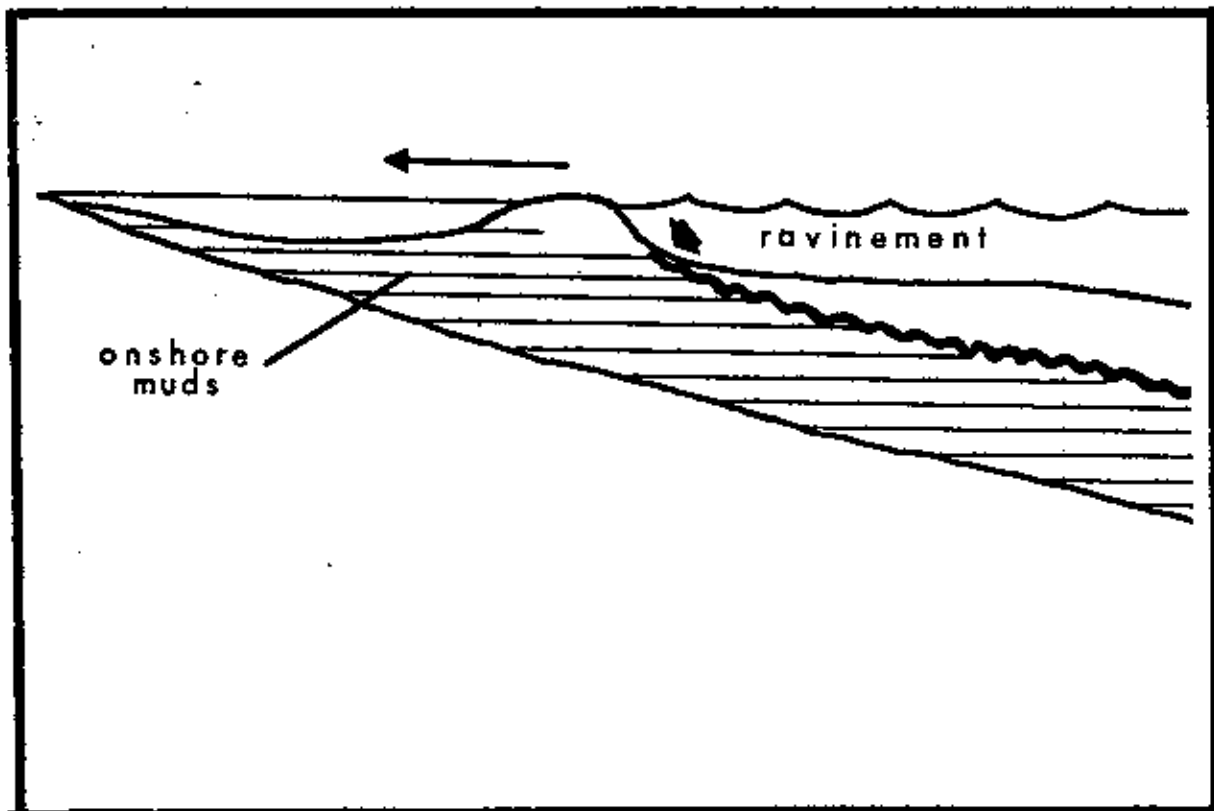
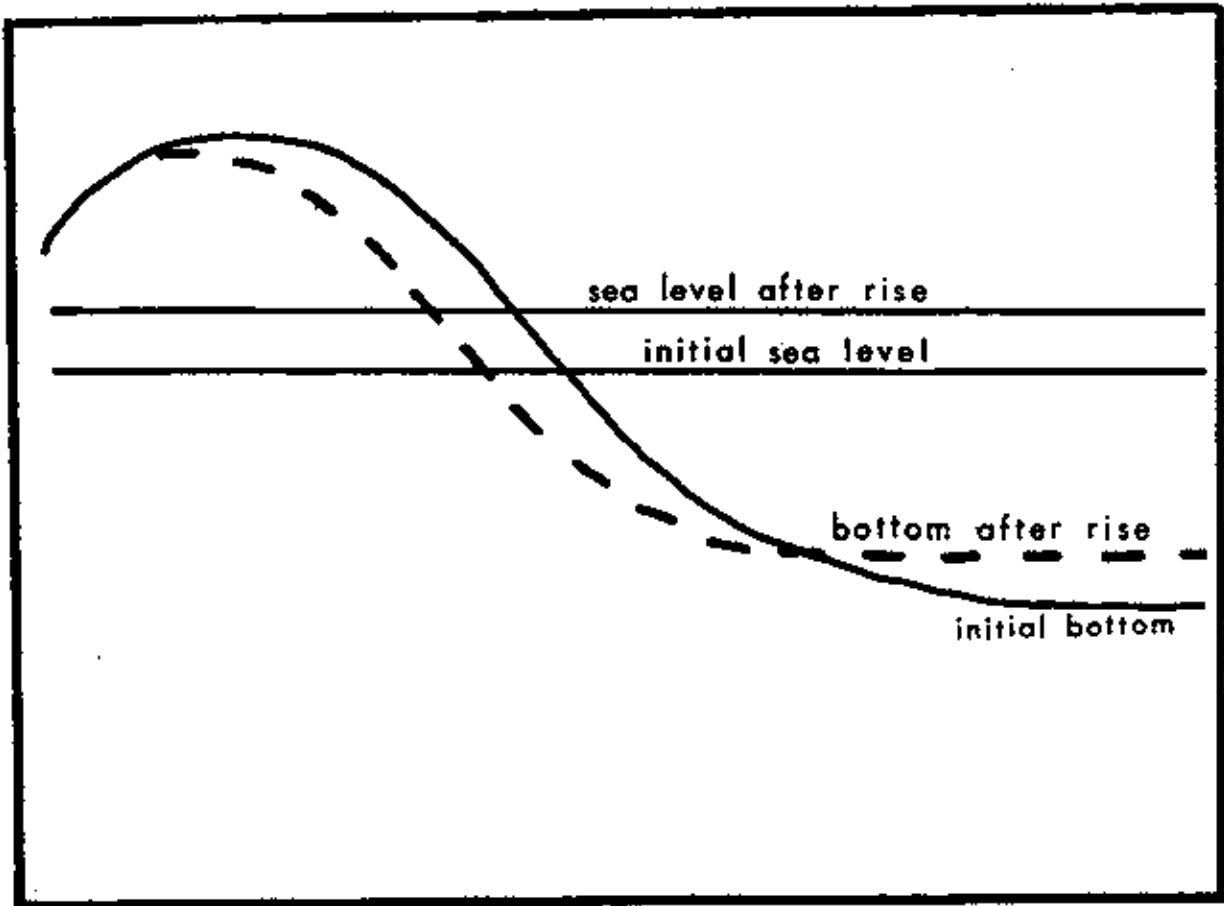


A detailed analysis of the erosional nature of the Manlius-Coeymans contact working under gradualistic assumptions was presented by Anderson (1972). He argued that the contact is a ravinement (figure 4), a discontinuity surface produced by shore-face erosion of a migrating barrier system with a rise in sea-level (Fischer, 1961; Swift, 1968). Explaining erosion at the formational boundary as the result of migration of the high energy Coeymans environment over the low energy Manlius environment, Anderson (1972) proposed a specific mechanism for the erosion evident at the contact in the Hudson Valley in a manner consistent with the basic assumptions underlying the prevalent gradualistic stratigraphic model.

In a recently published article, Anderson, Goodwin and Sobieski (1984) have questioned the validity of the assertion that Helderberg formational boundaries are actual diachronous surfaces separating paleoenvironmental units (p. 12). Detailed field observation indicated that most formation boundaries in the Helderberg sequence mark sharp contacts between markedly different facies. Because these facies are generally not transitional in lithological characteristics, they cannot represent laterally contiguous environments. Therefore, Helderberg formations could not have been deposited in response to lateral migration with gradual base-level rise. The sharp formational contacts are, however, consistent with the tenets of the hypothesis of punctuated aggradational cycles (PACs), a model of episodic accumulation which predicts abrupt facies changes at strati-

Figure 4a:  
Schematic representation of the ravinement  
process. After Fischer (1961).

Figure 4b:  
Ravinement concept as applied to the Manlius-  
Coeymans formational boundary. After Ander-  
son (1972).





graphic discontinuities.

According to the hypothesis of punctuated aggradational cycles (Goodwin and Anderson, 1980), stratigraphic accumulation occurs as thin (1-5 meter thick) shallowing-upward cycles (PACs) which are bounded by sharply defined non-depositional surfaces (figure 5). These surfaces are produced by geologically instantaneous, basin-wide base-level rises. Deposition between punctuation events occurs during periods of base-level stability. Because PACs are the products of these instantaneous basin-wide events, they are time-stratigraphic units which are laterally traceable through variable lithofacies and across diachronous formational boundaries (figure 6).

PACs occur in asymmetric deepening and shallowing sequences. According to the PAC hypothesis, these sequences are time-stratigraphic units produced by basin-wide synchronous patterns of punctuation events. Because they reflect pervasive vertical facies patterns on a scale larger than individual PACs, PAC sequences are useful as a means to correlate widely-spaced outcrops between which facies may change significantly.

### Objectives

This study is an attempt to apply the PAC hypothesis to the Manlius-Coeymans formational boundary. In order to accomplish this purpose, it is necessary to satisfy the following objectives: 1) to demonstrate that the upper portion of the Thacher Member of the Manlius Formation is completely divisible into PACs; 2) to correlate individual up-

Figure 5:  
Diagrammatic representation of fundamental  
tenets of the hypothesis of Punctuated Ag-  
gradational Cycles. After Anderson and  
Goodwin (1980)

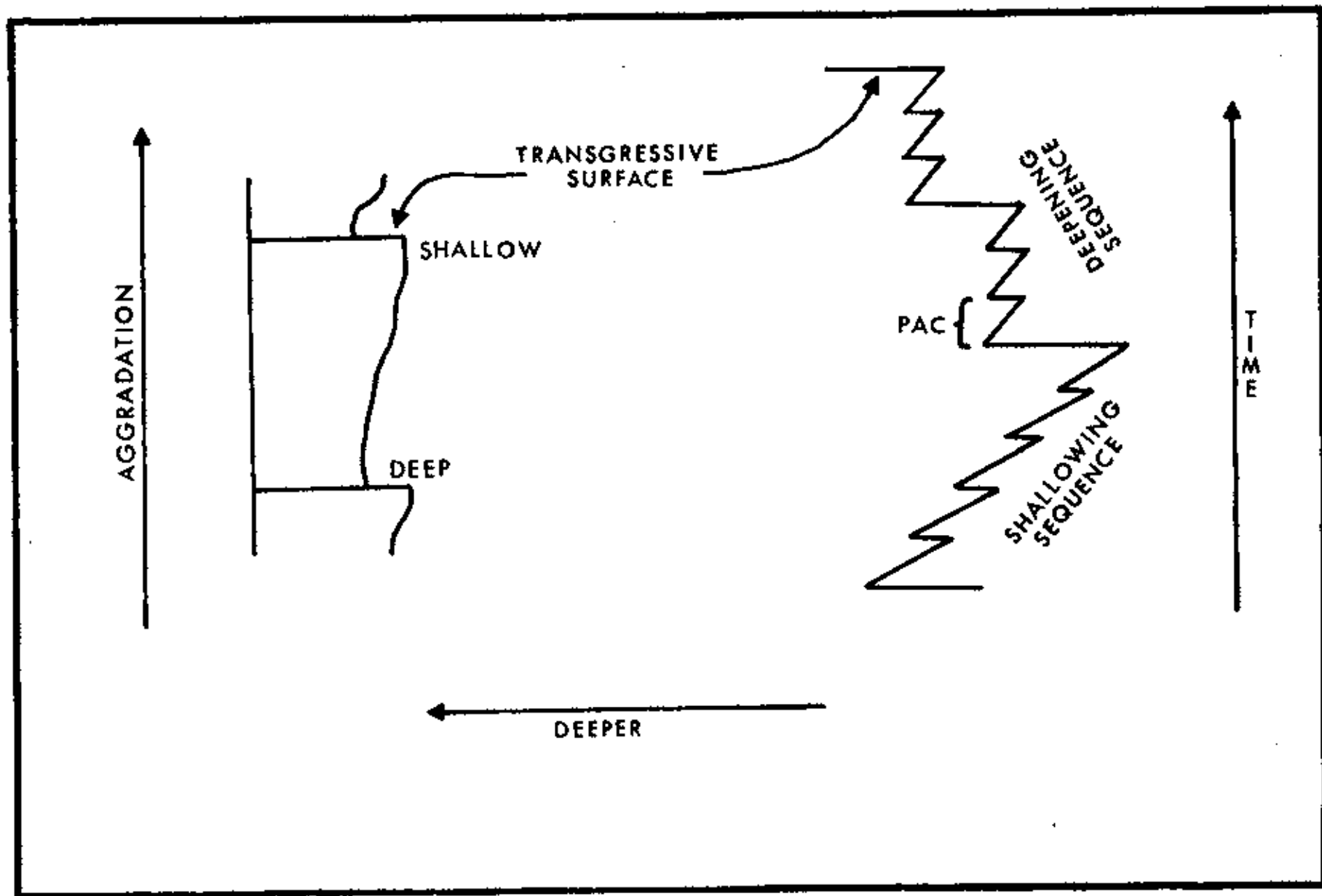
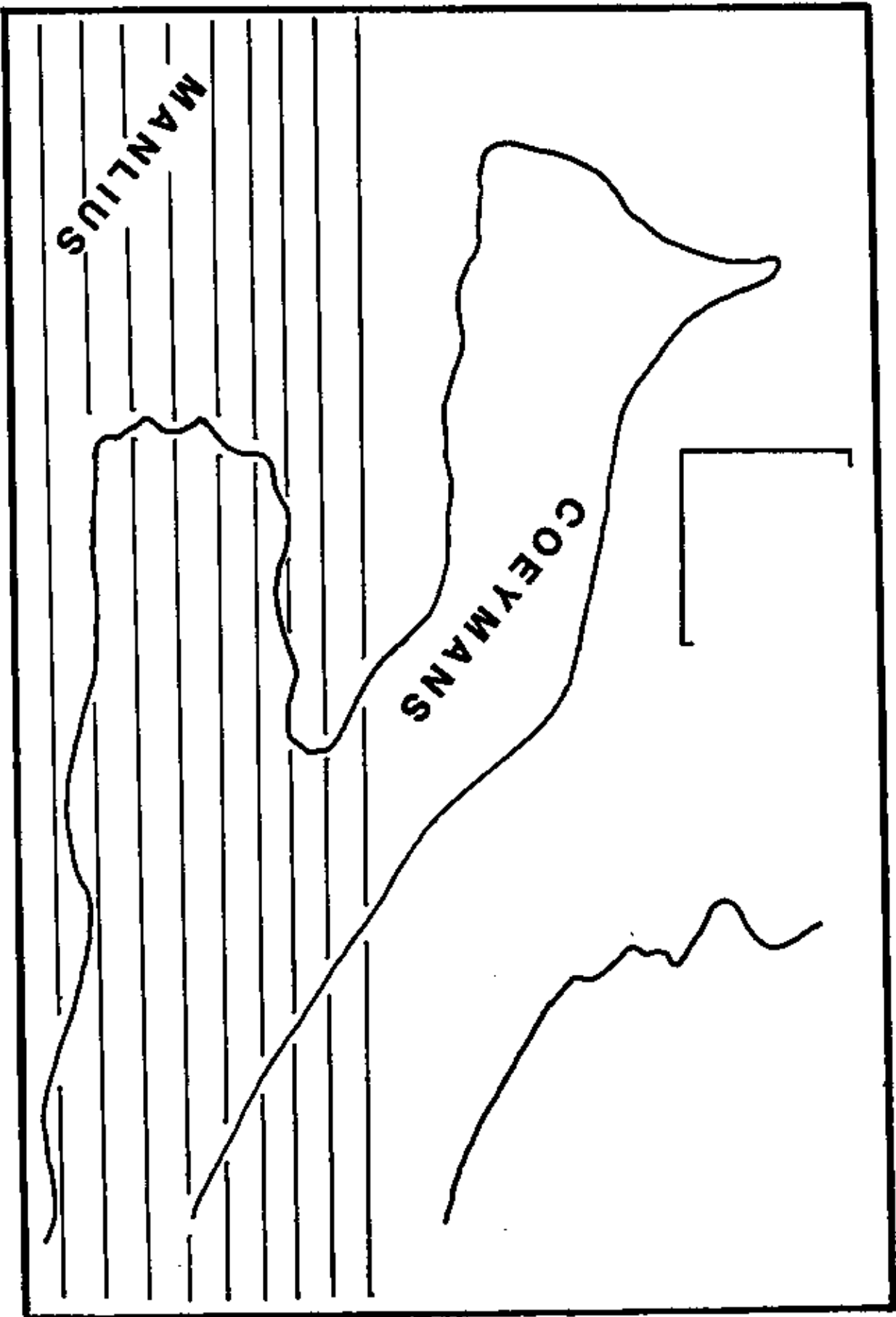


Figure 6:  
Illustration of the time-stratigraphic nature  
of PACs as compared to the diachroneity of  
traditional stratigraphic units. After (Ander-  
son and Goodwin, in press).







per Thacher PACs between localities; 3) to determine the lateral persistence and degree of preservation of uppermost Thacher PACs; and 4) to interpret the Manlius-Coeymans formational boundary as the product of one or more episodic base-level rises.

#### Methods

The PAC hypothesis, as an episodic model of stratigraphic accumulation, offers a new method of outcrop description and stratigraphic analysis (Goodwin et al., 1980). The PAC hypothesis states that deposition occurs in thin packages of facies which display a shallowing-upward motif. Application of this idea to field investigation changes the focus of data collection from rock-stratigraphic units (formations, members) to time-stratigraphic units (PACs, PAC sequences). This change in focus leads to different methods of subdividing and correlating a rock sequence.

At any single outcrop, field analysis involves the construction of a detailed stratigraphic column on graph paper at a scale of one inch to five feet of rock section. Special attention is given to vertical facies successions in the context of shallowing-upward cycles. Non-depositional surfaces between shallow facies below and deeper facies above mark PAC boundaries which are labeled on the constructed column. According to the PAC hypothesis, they are correlative, isochronous surfaces which can be traced basin-wide. As such, these surfaces provide the principle means of correlation from outcrop to outcrop.

Fieldwork for this study was accomplished during the





summers of 1982 and 1983. Stratigraphic columns were constructed for each of fourteen localities between Cherry Valley, New York, and South Wilbur, New York, a distance in excess of 100 kilometers along the outcrop belt (figure 7 foldout).

While facies changes in the Manlius Formation are generally discernible in the field, oriented whole-rock samples were collected for microscopic analysis at six key localities to support facies interpretations. Samples were taken directly above and below the Manlius-Coeymans contact, above and below each Manlius PAC boundary, and occasionally within PACs to obtain samples of the representative upper Thacher facies. Sixty thin sections were prepared from slabs cut normal to bedding. Samples were mounted on 75x38x1.00 mm petrographic glass slides with Conap epoxy adhesive and polished with 1000 mesh silicacarbide grit in the final polishing stage.



## MANLIUS FACIES AND PALEOENVIRONMENTS

In order to define PACs to be used in a stratigraphic analysis of the Manlius-Coeymans formational boundary, it is necessary to understand upper Thacher facies and to recognize persistent lateral and vertical facies patterns. Rickard, in his definitive reconstruction of Upper Cayugan and Helderbergian stratigraphy of New York State, recognized that, at its proposed type section, the Thacher Member of the Manlius is divisible into two parts: a lower 30 foot sequence consisting of relatively homogeneous facies, and an upper sequence about 20 feet thick containing variable lithologies. In the upper Thacher sequence, Rickard recognized three distinctive horizons: two stromatoporoid biostromes separated by a planar-laminated "waterlime" horizon. Rickard used the waterlime as a correlation datum on which to align stratigraphic columns from central New York and Hudson Valley localities. Although he considered them laterally discontinuous, Rickard also used the biostromes as a secondary means of correlation (1962, figure 2). Laporte (1967) recognized that the Manlius Formation is divisible into subtidal, intertidal and supratidal facies and that each was deposited at or near sea-level. In agreement with Rickard's observations, Laporte (1967) divided the Thacher Member into two parts according to sedimentary patterns. Laporte (p. 97) interpreted the lower sequence to consist mainly of intertidal facies and the upper sequence to be comprised primarily of supratidal and subtidal facies. As support for the use of the stromatoporoid biostromes for



making tentative correlations, Laporte (p. 85) noted that there are many places where the biostromes seem to be continuous for several miles.

Field observations of repetitive vertical sequences of subtidal, intertidal and supratidal facies are used to subdivide the Thatcher Member into eleven correlative PACs, each displaying a shallowing-upward motif. Each PAC contains facies which represent paleoenvironments present at a particular instant in Manlius time. Lateral facies variation within any stratigraphically equivalent PAC represents variation in coeval Manlius paleoenvironments (Saraka and Goodwin, 1984). Lateral facies changes are to be expected since modern analogues to the Manlius depositional environment often contain considerable variation in sedimentation and water depth from shoreline progressively offshore (Shinn et al., 1969) as well as parallel to the shoreline. The environments represented within any one PAC are newly created and separate from environments contained in preceding PACs. This does not imply, however, that there is no influence on facies in one PAC from accumulation in the preceding PAC. As noted by Saraka (1984), topographic relief on the top of a preceding cycle partially limits the facies which may develop in the PAC then aggrading (see PACs 6 and 9).

In this section, facies which occur in the upper Thatcher (figure 8) are described, illustrating their characteristic sedimentary structures and faunal assemblages.

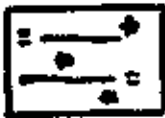
Figure 8:  
Legend for stratigraphic columns  
presented in figure 7.





# MANLIUS FACIES

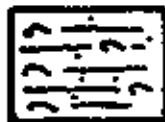
Shallowest



Birdseye Mud



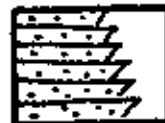
Cryptalgal Laminite



Ostracode Calcarenite



Ribbon Bed



Thin-bedded Calcarenite



Massive Calcarenite



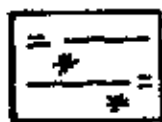
Biostrome



Medium-bedded Calcarenite

Deepest





The birdseye mud facies occurs both as sets of thin, light to medium gray beds separated by buff-colored laminated shales and as light to medium gray massive crinkle-textured beds (figure 9). Clasts, similar to those which have been compared to modern soil peds by Fischer (1975) are common in this facies. Fossils are rare except for an occasional disarticulated ostracode valve or thin lens of shell hash. This facies is well-developed in PAC 6 at Catskill localities and in PAC 7 at Kingston.

The birdseye mud facies is interpreted as a supratidal deposit. Birdseye fenestra have been interpreted as shrinkage pores which form during subaerial exposure (Laporte, 1967). Modern birdseye muds have been reported forming on tidal flats of the Bahamas (Shinn et al., 1969) and south Florida (Ginsburg, 1964) where the laminated facies develops on beach ridges and the unlaminated muds accumulate in tidal ponds. Analogous ancient facies have been described by Fischer (1964) from the Triassic of the Northern Alps and by Read and Grover (1977) from the Ordovician of Virginia.



The cryptalgal laminite facies forms buff-colored blocky units (figure 10), the massive appearance of which often being disrupted by columnar desiccation joints. This facies consists of alternating mm-scale beds of lime mud and microcrystalline dolomite. The micritic laminae commonly contain birdseye structures, and as with the birdseye mud facies, fossils are rare except for comminuted skeletal debris. This facies forms a laterally extensive horizon at the

Figure 9a:  
Supratidal birdseye mud facies, PAC 7  
at Kingston. White portion of stick  
is one foot in length.

Figure 9b:  
Thin-section photonegative of supratidal  
birdseye mud facies, PAC 6 at North Cat-  
skill. Scale in millimeters.



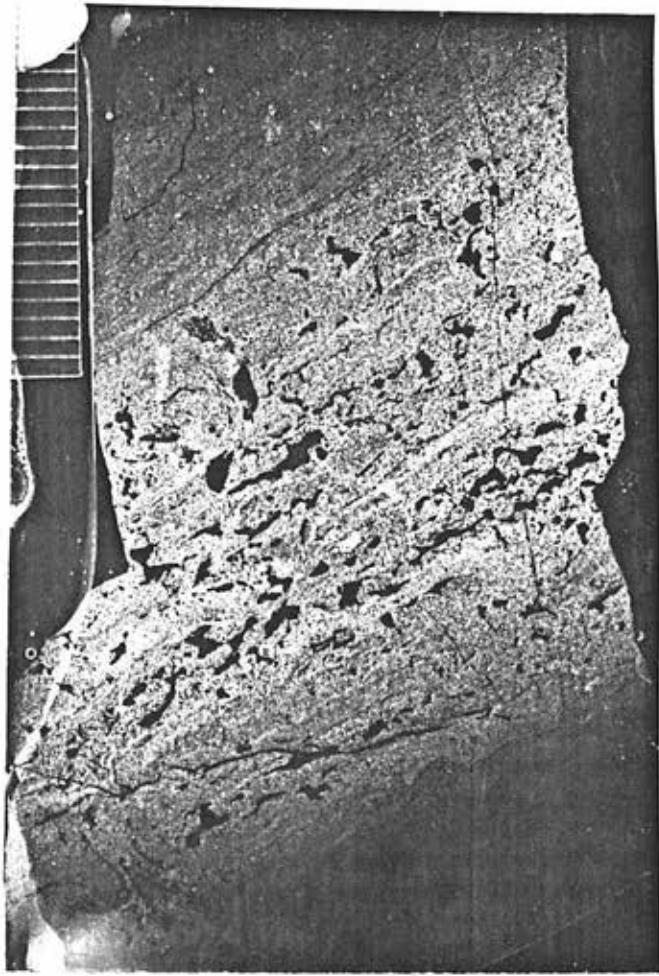
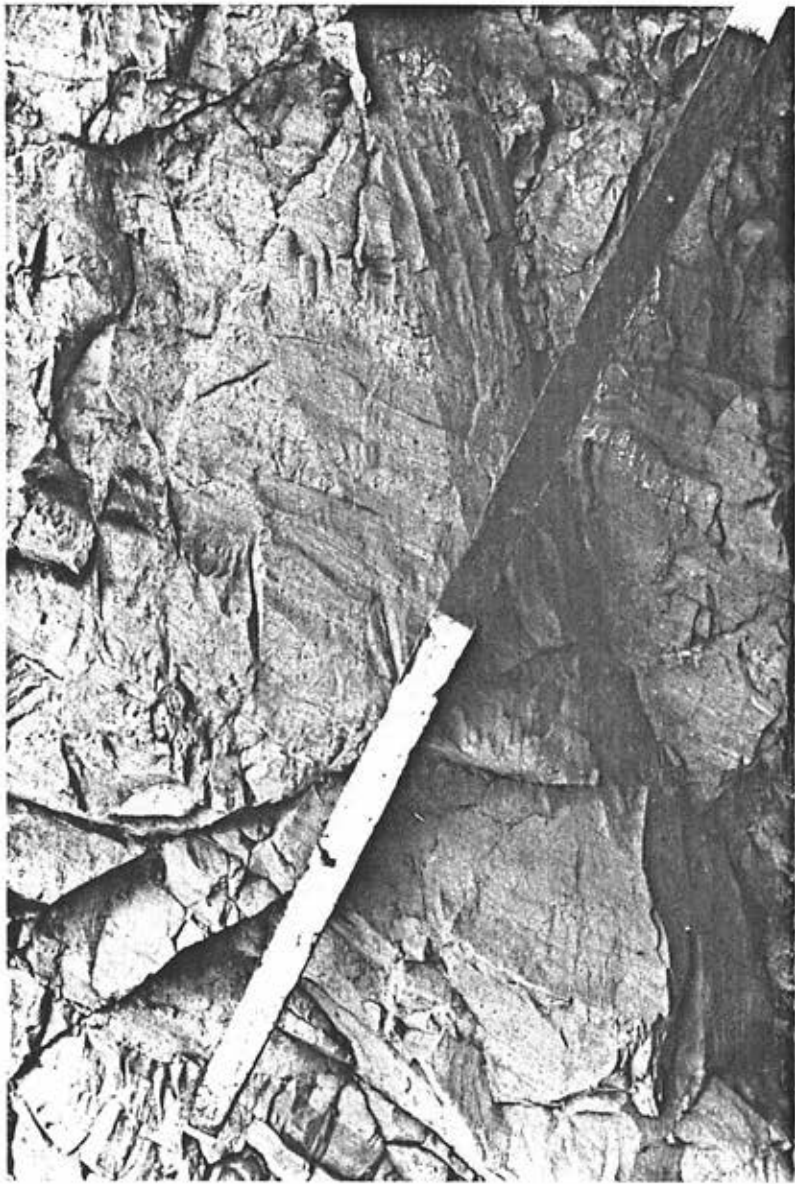
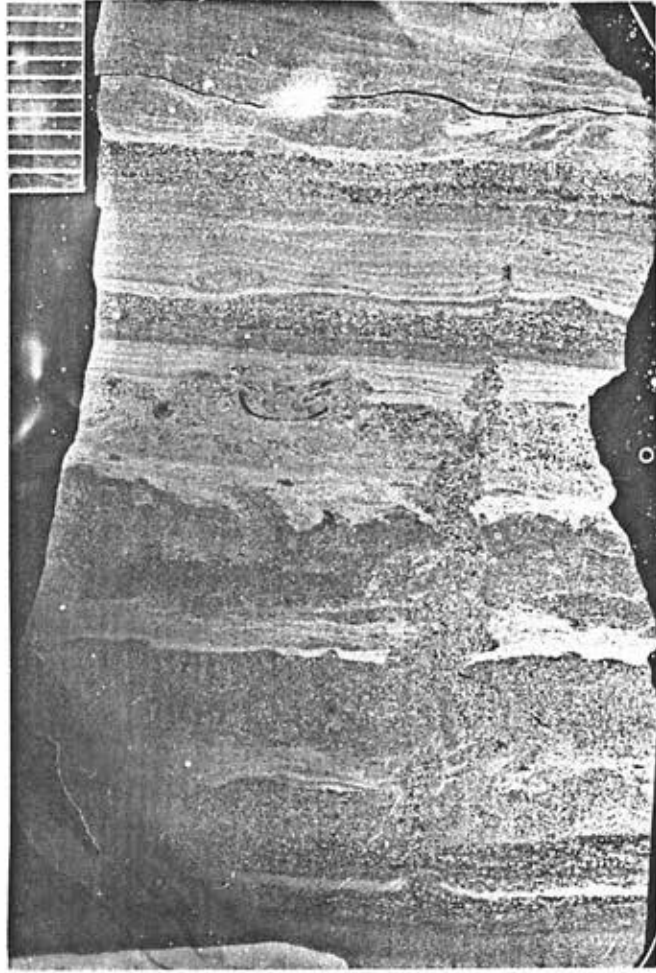
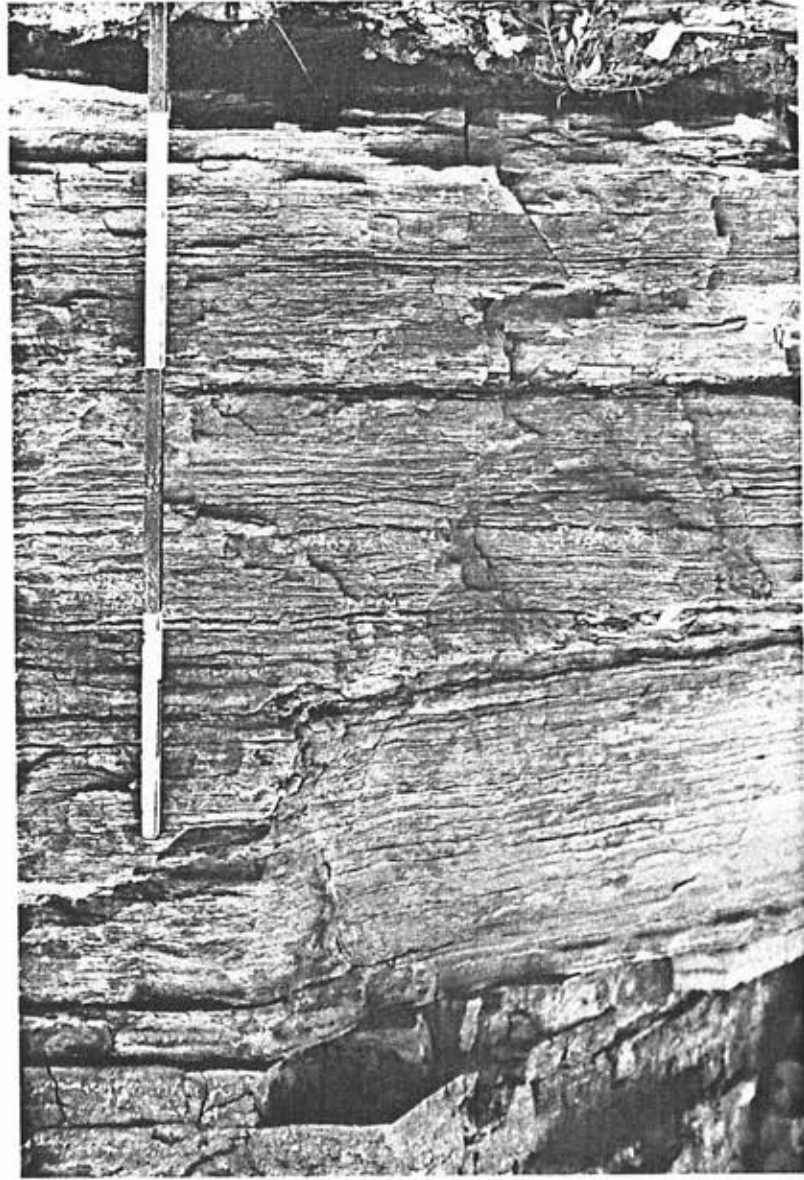


Figure 10a:  
Cryptalgal laminite facies, PAC 8 at Cherry  
Valley. Stick colored in one foot increments.

Figure 10b:  
Thin-section photonegative of cryptalgal  
laminite facies, PAC 8 at South Catskill.  
Scale in millimeters.

1 2 3 4 5 6 7 8 9 10 11 12 13 14 15 16 17 18 19 20 21 22 23 24 25 26 27 28 29 30 31 32 33 34 35 36 37 38 39 40 41 42 43 44 45 46 47 48 49 50 51 52 53 54 55 56 57 58 59 60 61 62 63 64 65 66 67 68 69 70 71 72 73 74 75 76 77 78 79 80 81 82 83 84 85 86 87 88 89 90 91 92 93 94 95 96 97 98 99 100 101 102 103 104 105 106 107 108 109 110 111 112 113 114 115 116 117 118 119 120 121 122 123 124 125 126 127 128 129 130 131 132 133 134 135 136 137 138 139 140 141 142 143 144 145 146 147 148 149 150 151 152 153 154 155 156 157 158 159 160 161 162 163 164 165 166 167 168 169 170 171 172 173 174 175 176 177 178 179 180 181 182 183 184 185 186 187 188 189 190 191 192 193 194 195 196 197 198 199 200 201 202 203 204 205 206 207 208 209 210 211 212 213 214 215 216 217 218 219 220 221 222 223 224 225 226 227 228 229 230 231 232 233 234 235 236 237 238 239 240 241 242 243 244 245 246 247 248 249 250 251 252 253 254 255 256 257 258 259 260 261 262 263 264 265 266 267 268 269 270 271 272 273 274 275 276 277 278 279 280 281 282 283 284 285 286 287 288 289 290 291 292 293 294 295 296 297 298 299 300 301 302 303 304 305 306 307 308 309 310 311 312 313 314 315 316 317 318 319 320 321 322 323 324 325 326 327 328 329 330 331 332 333 334 335 336 337 338 339 340 341 342 343 344 345 346 347 348 349 350 351 352 353 354 355 356 357 358 359 360 361 362 363 364 365 366 367 368 369 370 371 372 373 374 375 376 377 378 379 380 381 382 383 384 385 386 387 388 389 390 391 392 393 394 395 396 397 398 399 400 401 402 403 404 405 406 407 408 409 410 411 412 413 414 415 416 417 418 419 420 421 422 423 424 425 426 427 428 429 430 431 432 433 434 435 436 437 438 439 440 441 442 443 444 445 446 447 448 449 450 451 452 453 454 455 456 457 458 459 460 461 462 463 464 465 466 467 468 469 470 471 472 473 474 475 476 477 478 479 480 481 482 483 484 485 486 487 488 489 490 491 492 493 494 495 496 497 498 499 500 501 502 503 504 505 506 507 508 509 510 511 512 513 514 515 516 517 518 519 520 521 522 523 524 525 526 527 528 529 530 531 532 533 534 535 536 537 538 539 540 541 542 543 544 545 546 547 548 549 550 551 552 553 554 555 556 557 558 559 560 561 562 563 564 565 566 567 568 569 570 571 572 573 574 575 576 577 578 579 580 581 582 583 584 585 586 587 588 589 590 591 592 593 594 595 596 597 598 599 600 601 602 603 604 605 606 607 608 609 610 611 612 613 614 615 616 617 618 619 620 621 622 623 624 625 626 627 628 629 630 631 632 633 634 635 636 637 638 639 640 641 642 643 644 645 646 647 648 649 650 651 652 653 654 655 656 657 658 659 660 661 662 663 664 665 666 667 668 669 670 671 672 673 674 675 676 677 678 679 680 681 682 683 684 685 686 687 688 689 690 691 692 693 694 695 696 697 698 699 700 701 702 703 704 705 706 707 708 709 710 711 712 713 714 715 716 717 718 719 720 721 722 723 724 725 726 727 728 729 730 731 732 733 734 735 736 737 738 739 740 741 742 743 744 745 746 747 748 749 750 751 752 753 754 755 756 757 758 759 760 761 762 763 764 765 766 767 768 769 770 771 772 773 774 775 776 777 778 779 780 781 782 783 784 785 786 787 788 789 790 791 792 793 794 795 796 797 798 799 800 801 802 803 804 805 806 807 808 809 810 811 812 813 814 815 816 817 818 819 820 821 822 823 824 825 826 827 828 829 830 831 832 833 834 835 836 837 838 839 840 841 842 843 844 845 846 847 848 849 850 851 852 853 854 855 856 857 858 859 860 861 862 863 864 865 866 867 868 869 870 871 872 873 874 875 876 877 878 879 880 881 882 883 884 885 886 887 888 889 890 891 892 893 894 895 896 897 898 899 900 901 902 903 904 905 906 907 908 909 910 911 912 913 914 915 916 917 918 919 920 921 922 923 924 925 926 927 928 929 930 931 932 933 934 935 936 937 938 939 940 941 942 943 944 945 946 947 948 949 950 951 952 953 954 955 956 957 958 959 960 961 962 963 964 965 966 967 968 969 970 971 972 973 974 975 976 977 978 979 980 981 982 983 984 985 986 987 988 989 990 991 992 993 994 995 996 997 998 999 1000





top of PAC 8 which provides the major time and environmental datum in the upper Thacher. This datum corresponds to the waterline datum of Rickard (1962, figure 2). The eastern and western parts of Rickard's datum are linked in the Schoharie Valley by correlation of the algal and current laminites of other localities with a highly stylotized 2-3 inch, buff-colored laminated lime mud at Schoharie.

The cryptalgal laminite facies is interpreted as representing high intertidal conditions analogous to the flat and polygonal zone facies of modern Persian Gulf tidal flats (Kendall and Skipwith, 1968). Similar ancient facies have been described by Aitken (1967) from the Cambro-Ordovician of the southern Canadian Rockies and by Read (1973) from the Devonian of Western Australia.

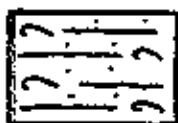
Gebelein and Hoffman (1973) have proposed that the presence of algae in the primary sedimentary environment plays an important role in the formation of secondary microcrystalline dolomite. They suggested that during deposition on algal-dominated tidal flats,  $Mg^{2+}$  is organically complexed in algal mats. Only after complete decomposition, which may not occur until burial and lithification, does the mat material release the magnesium required for dolomitization. Thus, in ancient cryptalgal laminite facies, algal mats are preserved as microcrystalline dolomitic laminae.

Research on the electrochemical interaction between clays and algae by Avnimelech and Troeger (1982) adds credibility to this hypothesis. In the presence of sufficient concentrations of  $CaCl_2$  or  $NaCl$ , algal-clay aggregates have

been experimentally flocculated and removed from suspension, effectively clarifying the water column. Avnimelech and Troeger (p. 63) suggest that

these interactions may profoundly affect the ecological structure of bodies of water in terms of the temporal and spatial distribution of organisms, the concentration of suspended inorganic particles and nutrients, nutrient recycling, substrate utilization by filter feeding organisms, and other processes.

It is worthy of note that Manlius dolomite beds are generally more argillaceous than Manlius lime units (Laporte, 1967), and that within the same PAC, the algal-dominated intertidal facies is sometimes dolomitized while the capping supratidal birdseye mud facies is not as in PAC 8 at North Catskill. Thus, the entrapment of clay-size particles by mucilaginous algal mats and the flocculation of algal-clay aggregates may have been primary processes which have led to the formation of secondary microcrystalline dolomite in the Manlius tidal flat facies.



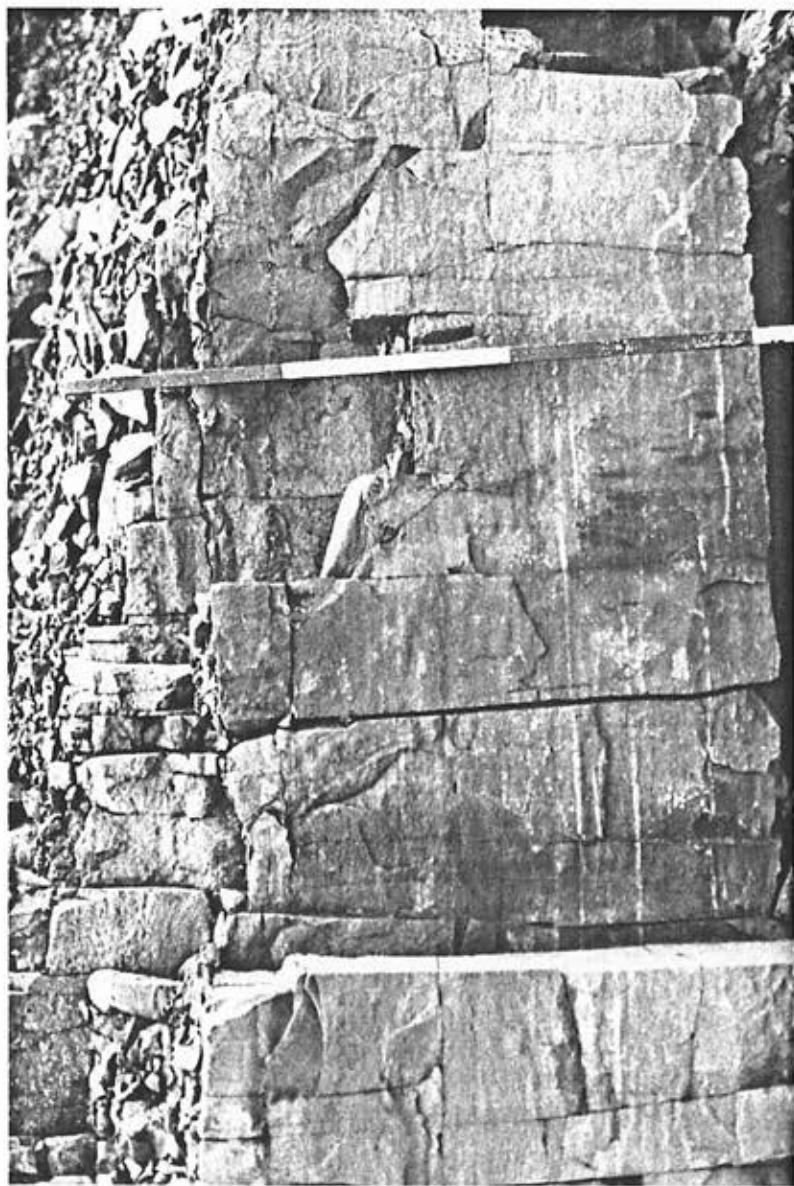
The ostracode calcarenite facies occurs as buff-colored blocky beds (figure 11). This facies consists of planar-laminated or low-angle cross-bedded pelletal sand with disarticulated leperditid ostracode valves most commonly oriented convex-upward. Laminae often have a crinkled texture suggestive of some algal influence on bedform.

The ostracode calcarenite facies is interpreted as representing a low intertidal carbonate bank environment. This facies shows no evidence of subaerial exposure; the fine lam-

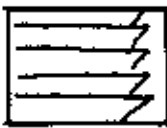
Figure 11a:  
Ostracode calcarenite facies, PAC 5  
at Schoharie. Stick colored in one  
foot increments.

Figure 11b:  
Thin-section photonegative of ostracode  
calcarenite facies, PAC 9 at Cherry Valley.  
Scale in millimeters.

1  
2  
3  
4  
5  
6  
7  
8  
9  
10  
11  
12  
13  
14  
15  
16  
17  
18  
19  
20  
21  
22  
23  
24  
25  
26  
27  
28  
29  
30  
31  
32  
33  
34  
35  
36  
37  
38  
39  
40  
41  
42  
43  
44  
45  
46  
47  
48  
49  
50  
51  
52  
53  
54  
55  
56  
57  
58  
59  
60  
61  
62  
63  
64  
65  
66  
67  
68  
69  
70  
71  
72  
73  
74  
75  
76  
77  
78  
79  
80  
81  
82  
83  
84  
85  
86  
87  
88  
89  
90  
91  
92  
93  
94  
95  
96  
97  
98  
99  
100



ination and low angle cross-bedding are suggestive of low energy swash of small mud clasts, fecal pellets and delicate bioclasts which comprise this facies. The remarkable lateral persistence of this facies as evident in PAC 6 suggests that Manlius carbonate banks were probably as large as Holocene mudbanks in the Florida reef tract described by Turmel and Swanson (1976).



The ribbon bed facies occurs as light gray, one to two inch beds separated by thin buff-colored argillaceous shale (figure 12). Beds consist of pelloids and are most commonly graded or contain wispy cross-beds. The bases of individual ribbons may display erosional relief; the tops of ribbons are generally planar or gently rippled. Most often, beds are internally barren of body fossils, but a lag of shell hash may occur at the base of some beds. In contrast to the internal paucity of fossils, a fauna rich in numbers but low in diversity litters the bedding planes. The bedding plane assemblage includes leperditid ostracodes (Hermannina alta), spiriferid brachiopods (Howellella vanuxemi), tentaculites (Tentaculites gyraacanthus), unidentified trepostome bryozoans and an occasional clam (Laporte, 1967). Algal thrombolites also occasionally occur in the ribbon bed facies. Although they weather the same color as the ribbons, they are discernible by their clotted fabric and the disruption of bedding.

The Manlius ribbon facies is interpreted as representing a shallow subtidal lagoonal environment. Ribbons may be

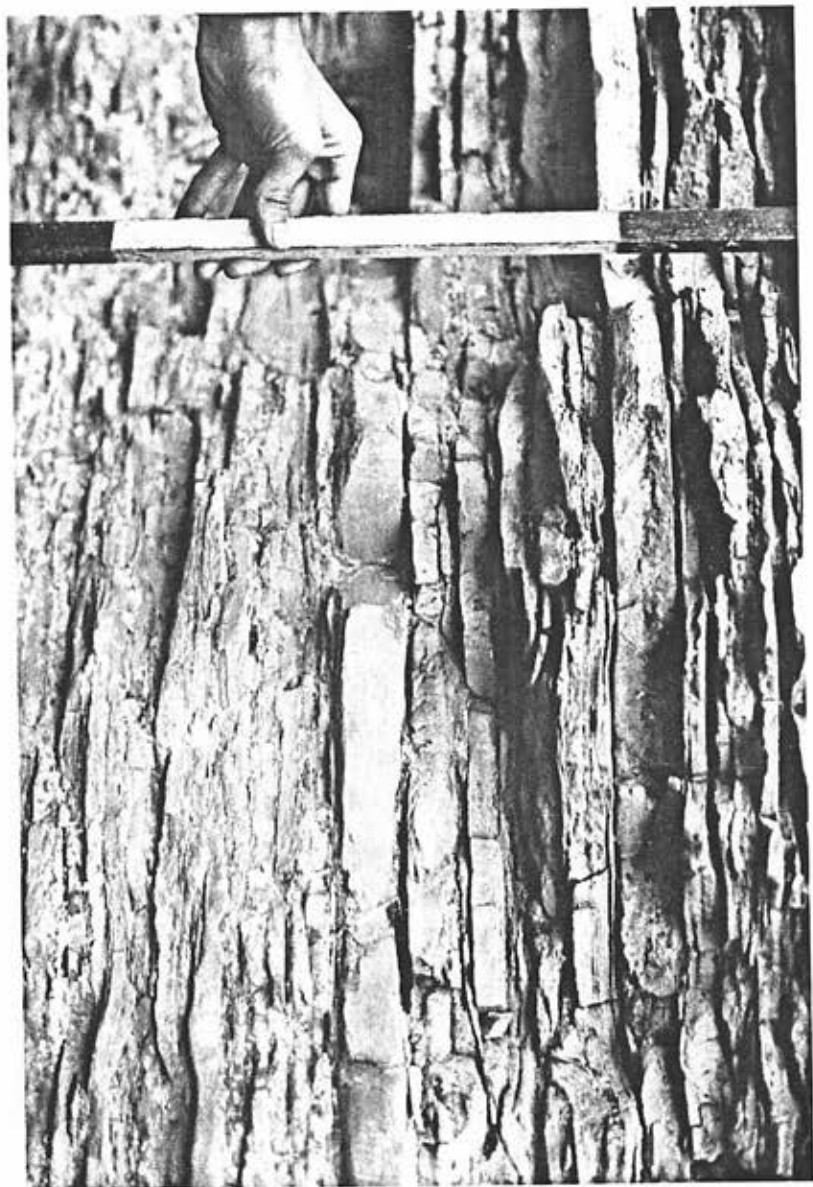
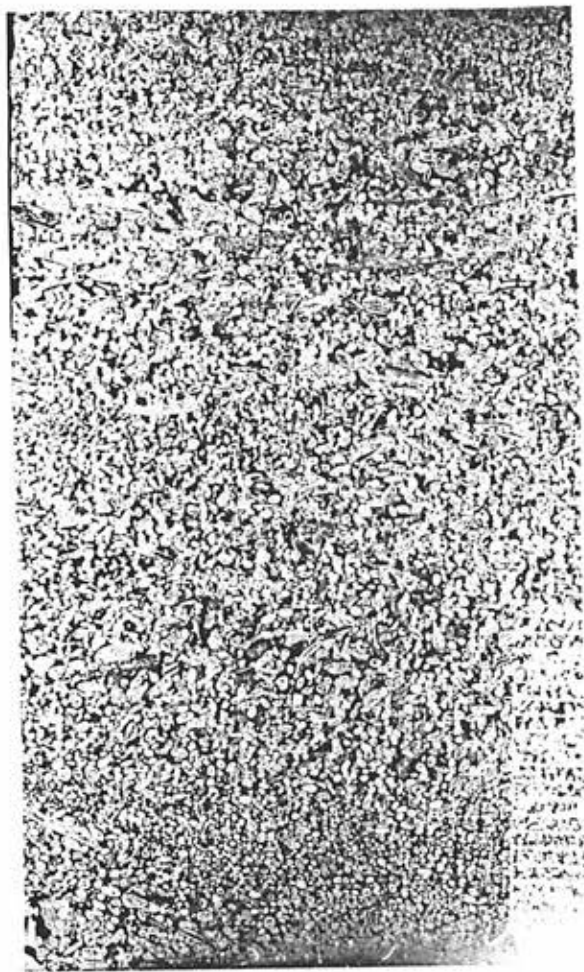




Figure 12a:  
Ribbon bed facies, PAC 5 at Thacher Park.  
White portion of stick is one foot in  
length.

Figure 12b:  
Thin-section photonegative of ribbon bed  
facies, PAC 8 at Schoharie. Scale in  
millimeters.





storm-generated beds which introduced carbonate sediment into an otherwise low energy, sediment starved environment. The prolific population of brachiopods and other body fossils that this facies supports that Manlius ribbons are predominantly subtidal as opposed to the intertidal interpretation presented by Laporte (1967). Manlius ribbons generally do not display any evidence of subaerial exposure (i.e. dessication cracks). However, as aggradation continues beyond the subtidal phase, ribbons grade vertically into intertidal facies exhibiting decreasing bedding thickness and faunas, and increased evidence of scour and fill.

Although slightly different in composition, the ribbon facies described by Demicco (1983) and Read (1983) from the Cambrian Conococheague Formation of Virginia is considered analogous to the Manlius ribbon facies. The presence of dolomite interbeds, instead of argillaceous shale partings may reflect a greater algal influence in the Cambrian setting. Read (1983, p. 4) has noted algal thrombolites and digitate structures in the ribbon facies which supports this hypothesis. Gebelein and Hoffman (1973) have proposed that algae play a major role in the development of microcrystalline dolomite beds, and Avnimelech and Troeger (1982) have discussed the electrochemical flocculation of algae and clay. Therefore, the presence of dolomite in the Cambrian ribbon facies may not reflect a significantly different depositional environment.





The Manlius biostrome facies occurs as dark gray massive beds ranging from one foot to nearly six feet in thickness (figure 13). The biostromes are comprised of a single species of stromatoporoid, Syringostroma baretii, which forms spherical heads usually less than one foot in diameter. Interstitial pockets in the biostrome contain lime mud and codiacean algae (Laporte, 1963 and 1967) and support a relatively diverse fauna including several genera of ostracodes, loxonematid gastropods, solitary rugosan corals (Spongophylloides sp.) and strophomenid brachiopods (Mesodouvilina varistriata).

The stromatoporoid biostrome is a key facies in the upper Thacher forming two horizons which provide valuable markers for correlation. The stromatoporoids develop two laterally persistent biostromes, one in PAC 7 extending from Thacher Park to Kingston, a distance of approximately fifty-five miles, and one in PAC 8 extending from Thacher Park to Catskill, a distance of nearly thirty miles. The lateral and vertical gradation of these extensive biostromes into adjacent facies suggests that the buildups were significant contributors of sediment to other Manlius environments.

Manlius biostromes are different from other Devonian stromatoporoid buildups such as the Judy Creek Reef Complex of central Alberta (Wendte and Stoakes, 19 ) and those of the Pillara Formation of Western Australia (Read, 1973) in that <sup>they</sup> consist of only one species of stromatoporoid. Laporte (1967, p. 88) suggested that, unlike other species,

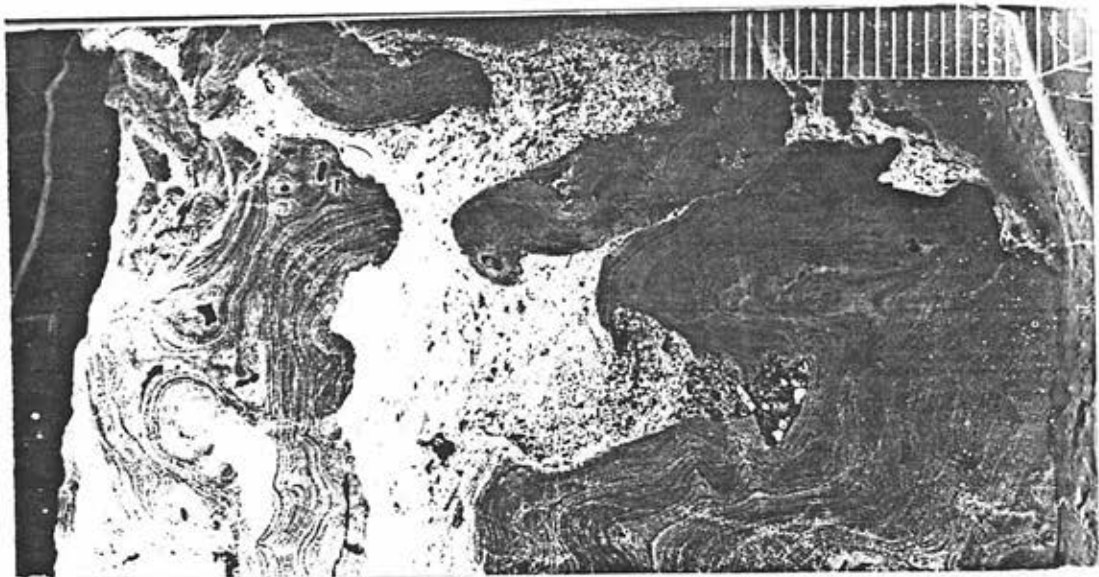
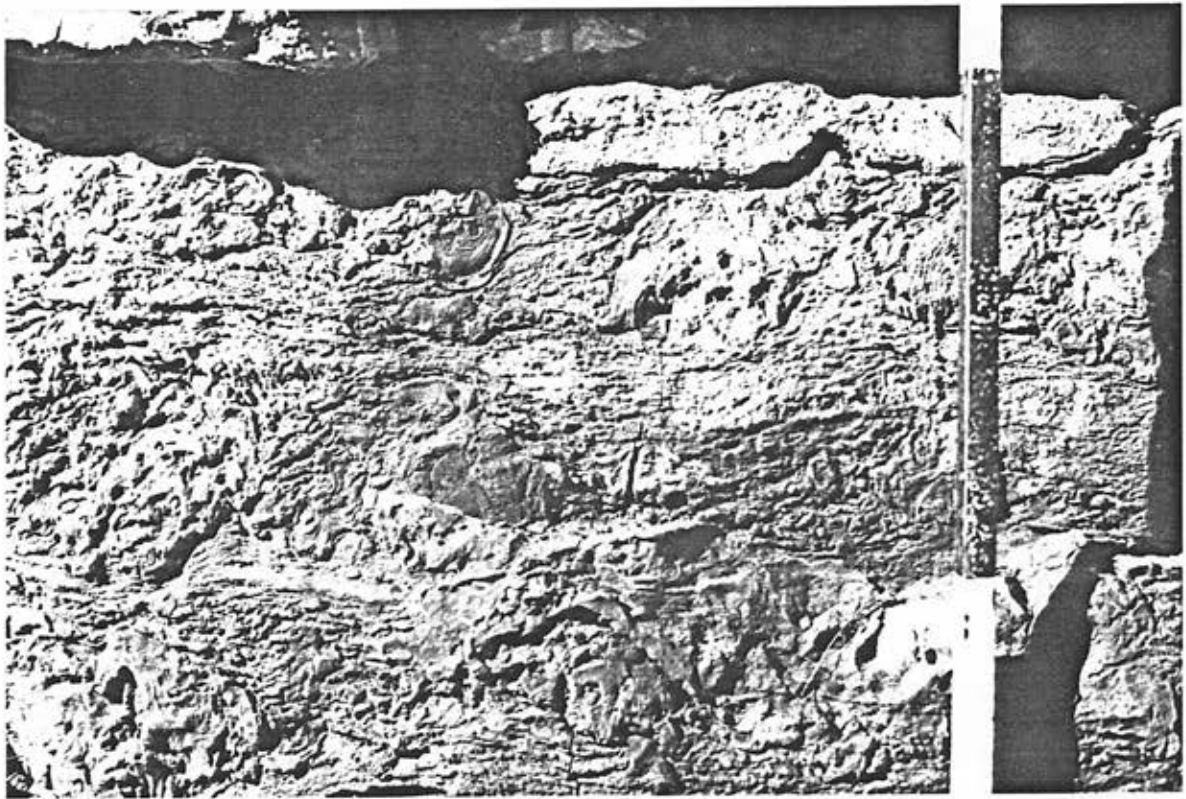


Figure 13a:  
Stromatoporoid biostrome facies, PAC 10  
at New Salem. Red portion of stick is  
one foot in length.

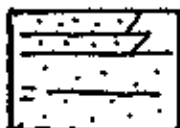
Figure 13b:  
Thin-section photonegative of stromatoporoid  
biostrome facies, PAC ? at New Salem.







Syringostroma barretti may have been tolerant of mud which probably clouded Manlius waters during periods of substrate disturbance.



Two types of calcarenite defined by faunas and bedding thickness dominate different stratigraphic intervals in the upper Thacher sequence. Where subtidal portions of PACs are not comprised exclusively of stromatoporoids, Manlius PACs 6-9 are dominated by thin-bedded calcarenite and a bioturbated equivalent. In Manlius PACs 10-11, which contain facies representing the deepest subtidal Thacher environments, medium-bedded calcarenite and its bioturbated equivalent occur in the absence of stromatoporoid biostromes. Although differences in the composition of these calcarenites appear slight, bedding thickness and the lateral and vertical gradation of the calcarenites into other facies provide information leading to the interpreted depth relationships.

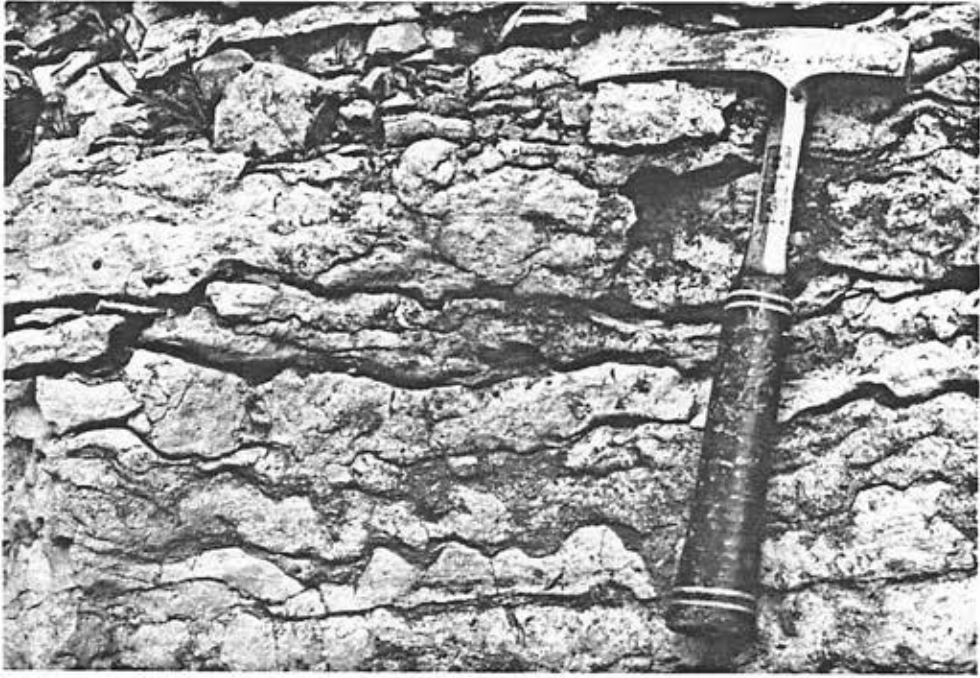
Shallow-water calcarenites occur in Manlius PACs 6-9. Thin-bedded and massive bioturbated calcarenite contain ostracodes, gastropods, spiriferid brachiopods (Howellella vanuxemi), and stromatoporoid fragments. The thin-bedded calcarenite occurs as two inch to four inch beds separated by thin, buff-colored shales (figure 14). The bedding thickness and the color of the shale interbeds reflect the laterally gradational relationship between this facies and the ribbon bed facies as seen in Manlius PACs 6 and 8.

Although no significant difference in water depth is

Figure 14a:  
Thin-bedded calcarenite facies, top of PAC 7  
at North Catskill.

Figure 14b:  
Thin-section photonegative of thin-bedded  
calcarenite facies, PAC 7 at East Kingston  
Quarry. Scale in millimeters.







inferred, the lateral facies distribution in Manlius PACs 6 and 8 also suggests some environmental significance to the presence of bioturbation in the shallow calcarenite facies. The bioturbated calcarenite seems to occur atop areas of low relief within the biostrome, whereas the thin-bedded facies is more well-developed at the biostrome margins. Thus, there exists a gradation in the bedding thickness, grain size, and degree of bioturbation from massive bioturbated bedding in the Manlius biostrome environment decreasing progressively through the biostrome margin and into the Manlius lagoonal environment.

One striking difference between the shallower calcarenite facies and the deeper facies is the color and content of shale. The medium-bedded calcarenite, interpreted as the deepest Manlius facies, occurs as five inch to eight inch beds often separated by unfossiliferous black shales up to two inches in thickness (figure 15). At localities where well-developed sequences of this facies are preserved (i.e. Schoharie) the medium-bedded calcarenite displays internal sedimentological changes that reflect shallowing-upward conditions. The basal portion of the sequences contain the thickest shales which decrease in thickness upward as carbonate beds amalgamate. These sequences are capped by massive bioturbated beds up to eighteen inches thick.

The most significant difference in composition between this facies and the shallower calcarenites is the addition of the strophomenid brachiopod, Mesodouvillina varistriata, along with the occurrence of small crinoid ossicles (figure

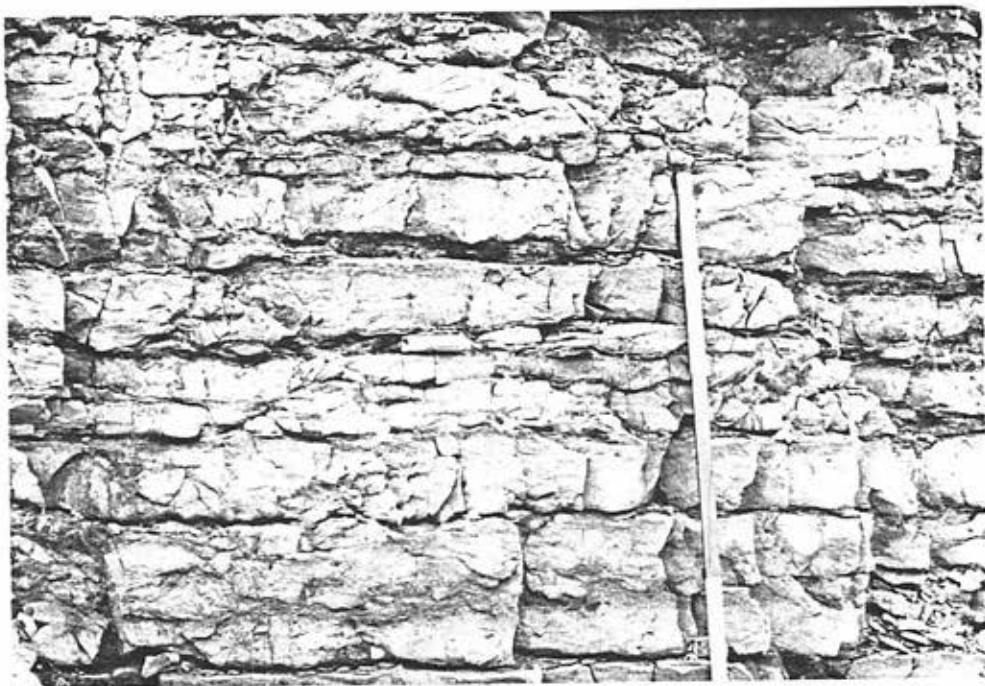




Figure 15a:  
Medium-bedded calcarenite facies, PAC 10 at  
Callanan Quarry. Stick is divided into one  
foot increments.

Figure 15b:  
Thin-section photonegative of medium-bedded  
calcarenite facies, PAC 11 at Cherry Valley.  
Scale in millimeters.





.....

.....

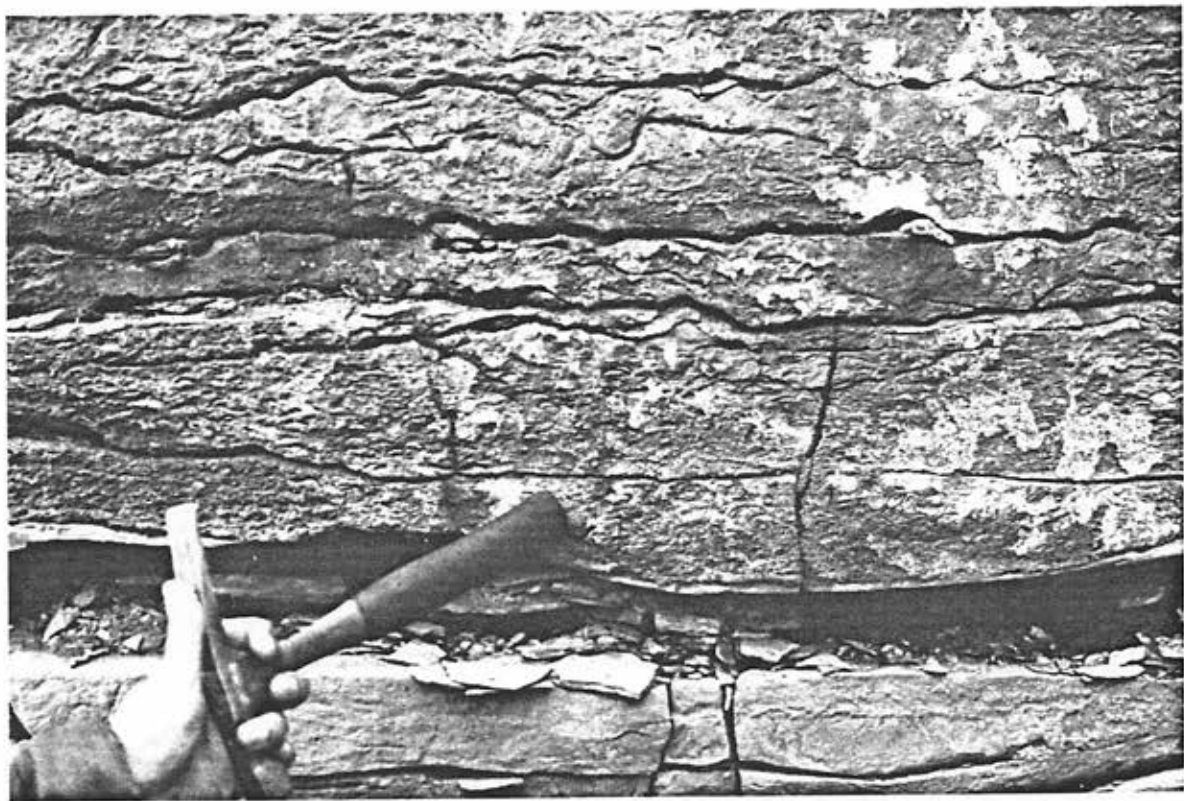
16). This is of significance, because Mesodouvillina is found at the top of the Thacher as far south as Catskill and is evidence that the medium-bedded facies extends farther south than earlier workers (i.e. Davis, 1953; Rickard, 1962) have contended. This suggests that the medium-bedded calcarenite facies was not a laterally transitional facies to the Coeymans Formation, but that it may have extended over much of the study area during late Thacher time only to be removed by subsequent pre-Coeymans erosion.



Figure 16:  
Strophomenid-bearing medium-bedded cal-  
carenite facies, top of PAC 11 at Schoharie.







## MANLIUS PACs

Laporte (1967), recognizing that the Manlius Formation is divisible into subtidal, intertidal and supratidal facies, interpreted the repetitive vertical succession of these facies as a complex mosaic resulting from the irregular migration of Manlius subenvironments. In contrast, this study suggests that the vertical repetition of facies patterns in PACs is an ordered response of Manlius subenvironments to allogenic processes, repeated small-scale base-level rises.

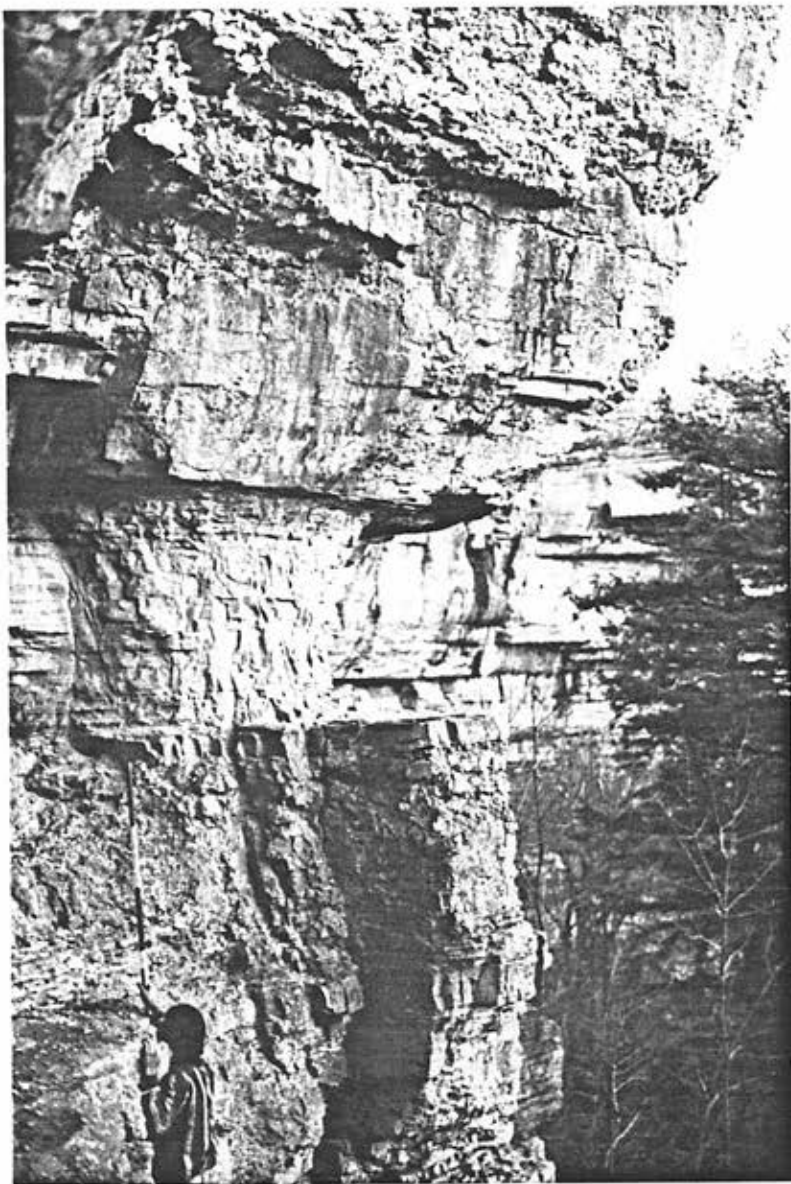
At each of 14 localities in central New York and the Hudson Valley, the Thacher Member of the Manlius Formation is completely divisible into PACs (figure 7). Each Manlius PAC has been assigned a number according to its fixed position within the vertical succession of cycles, so that at every locality where it is preserved, a correlative PAC retains the same number. The focus of this study is on PACs in the upper half of the Thacher Member (Manlius PACs 6-11). For discussion of PACs in the lower Thacher sequence, refer to Saraka (1984).

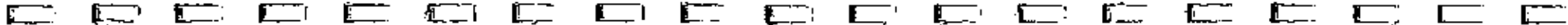
General Characteristics of Upper Thacher PACs

Two types of PACs occur in the upper Thacher sequence. Manlius PACs 6-9 are of the first type which consists of shallow subtidal through supratidal facies. A typical subtidal-to-supratidal PAC is PAC 8 at John Boyd Thacher Park (figure 17). At this locality, PAC 8 is 9 feet thick. At

Figure 17:  
Subtidal-to-supratidal PAC: PAC 8  
at John Boyd Thacher State Park.







its base, PAC 8 contains 1 foot of thin-bedded calcarenite containing abundant gastropods and ostracodes. This calcarenite is overlain by a well-developed 4 feet thick stromatoporoid biostrome. The biostrome is capped by a 6 inch lime mud bed which marks the transition from subtidal to intertidal facies. Directly overlying the lime mud bed is 6 inches of fine-grained, laminated ostracode calcarenite which records aggradation of sediment into the lower intertidal zone. Above the ostracode calcarenite there are 4 feet of planar algal laminites, the top 6 inches of which are polygonally mudcracked. The mudcracked laminites represent high intertidal to supratidal conditions and completes the series of facies from subtidal through supratidal typical of this kind of PAC.

In contrast to PACs 6-9, PACs 10 and 11 consist entirely of subtidal facies. PAC 10 at the Schoharie locality is a typical subtidal PAC (figure 18). At Schoharie, PAC 10 is 6.5 feet thick and is made up of 5 feet of medium-bedded calcarenite containing strophomenid brachiopods overlain by 1.5 feet of massive bioturbated calcarenite containing stromatoporoid fragments. This facies sequence indicates aggradation from relatively deep subtidal conditions to shallow subtidal conditions.

#### PACs in Columnar Section

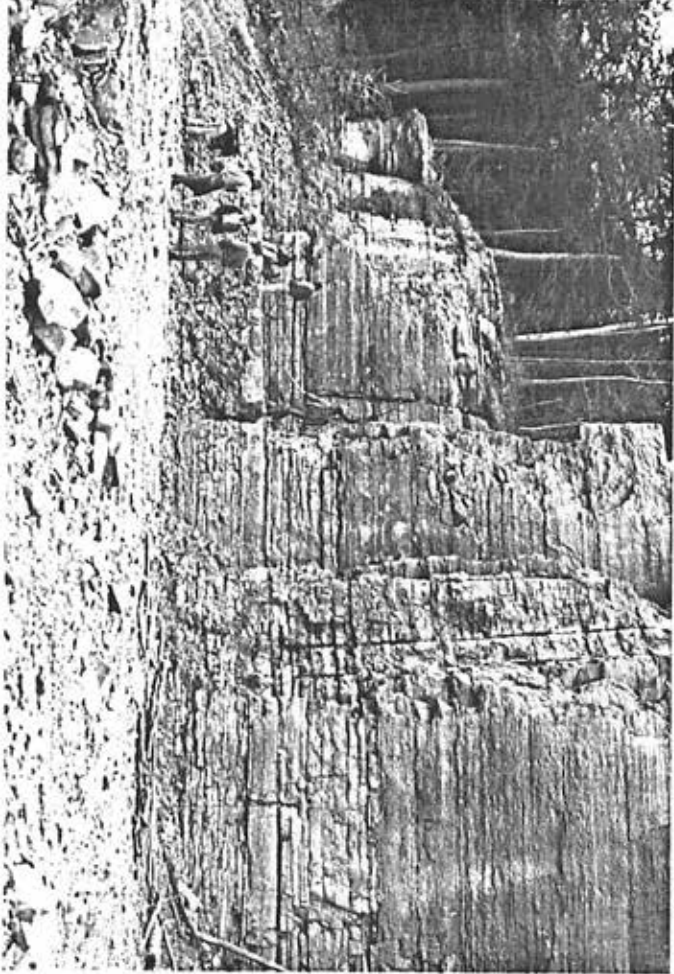
At its type section, John Boyd Thacher State Park, the Thacher Member of the Manlius Formation is divisible into 11 PACs. These PACs are organized into two sequences. PACs 1-5

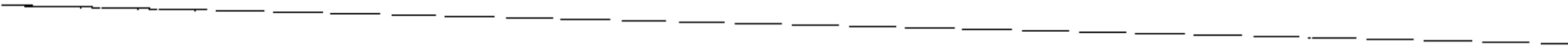
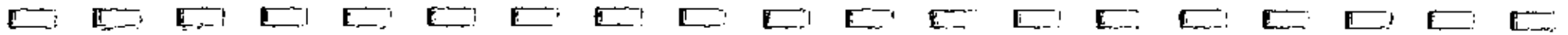


Figure 18:

Fully subtidal PAC: PAC 10 at Schoharie







comprise the lower sequence which is dominated by intertidal facies (Saraka, 1984). The upper sequence, PACs 6-11, is dominated by subtidal stromatoporoid-rich facies and is the focus of this study.

Deposition of the upper Thacher sequence was affected by both allogenic and autogenic processes which can be graphically represented by a relative water depth curve (figure 19). Rapid base-level rises which produce PAC boundaries are allogenic events and are represented by horizontal deflections of the curve. The magnitude of the change in sea-level is proportional to the size of the deflection. Gradual vertical aggradation of facies, an autogenic process, is indicated by diagonal lines. Vertical lines indicate the amount of stratigraphic accumulation attributable to gradual subsidence.

PAC 6, the basal cycle of the upper sequence, is a single-environment PAC (Saraka, 1984, p. 18) which consists entirely of current-laminated ostracode calcarenite. Shallowing in PAC 6 is indicated by progressive thinning and increased planar nature of individual laminae.

PAC 7 is 5.5 feet thick and contains one of four stromatoporoid horizons which occur in the Manlius at Thacher Park. Interbedded stromatoporoids and fossiliferous thin-bedded calcarenite form a sequence about four feet thick. This stromatoporoid facies is capped by 1.5 feet of current-laminated ostracode calcarenite.

PAC 8 (illustrated earlier) is 9 feet thick and displays aggradation of sediment from subtidal through supratidal con-

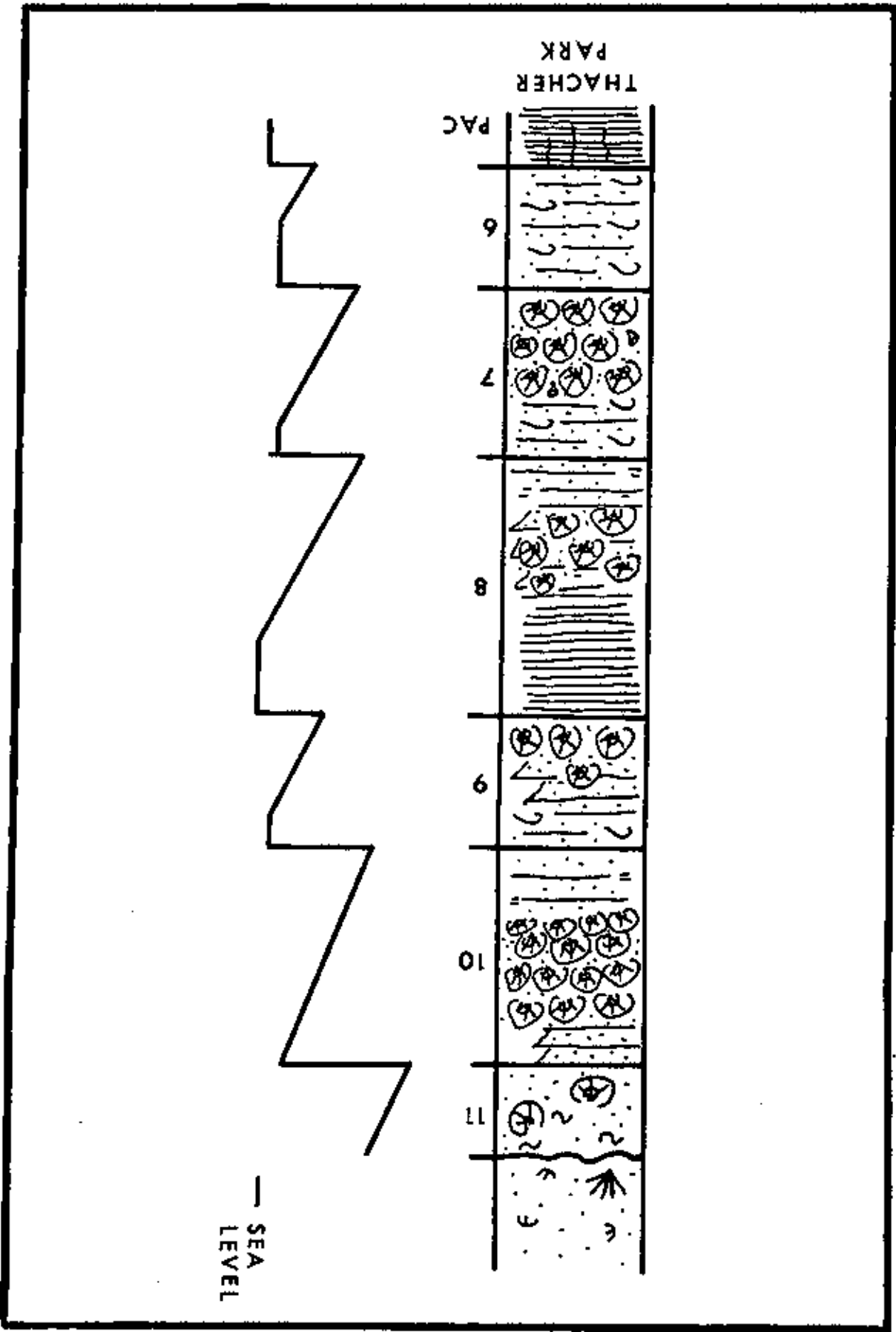


Figure 19:  
Stratigraphic column and interpreted relative  
water depth curve for upper Thacher sequence at  
the type section, John Boyd Thacher State Park.

Vertical line of marks on the left side of the page.

Vertical line of marks on the right side of the page.







ditions. The subtidal portion of this cycle, like that of PAC 7, is dominated by stromatoporoid facies. The PAC 8 biostrome, which is approximately 3 feet thick, is capped by a 4 foot thick sequence of algal laminites. This laminite horizon is the waterline datum of Rickard (1962, figure 2) at the Thacher type section.

PAC 9 is 4 feet thick and contains the third stromatoporoid horizon present at Thacher Park. PAC 9 stromatoporoids occur interbedded with medium- to thin-bedded calcarenites which represent subtidal conditions in PAC 9. Two feet of ostracode calcarenite accumulated over this third stromatoporoid horizon indicating shallowing upward to the intertidal zone.

PAC 10 is 7.5 feet thick and contains the fourth stromatoporoid horizon. At its base, PAC 10 contains 3 feet of medium-bedded calcarenite with shale interbeds. The PAC 10 biostrome, which is 4 feet thick, occurs at the top of the PAC. Thus, PAC 10 deposition was terminated under subtidal conditions.

PAC 11, which is 3.5 feet thick, is another single-environment PAC. PAC 11 consists of massive, bioturbated, crinoidal and strophomenid-bearing calcarenite. This lithosome was considered to be a Coeymans facies by Rickard (1962, p. 122). It is included in the Manlius by this author because of the presence of strophomenids and the absence of Gypidula coeymanensis. The PAC 11 strophomenid coquina-like facies is directly overlain by the coarse crinoidal and